

Controlling electronic properties of epitaxial nanocomposites of dissimilar materials

M.P. Hanson*, S.R. Bank, J.M.O. Zide, J.D. Zimmerman, A.C. Gossard

Materials Department, University of California, Santa Barbara 93106-5050, USA

Available online 23 January 2007

Abstract

The electronic properties of epitaxial semiconductors are strongly modified by the inclusion of semi-metallic nanoparticles grown in the semiconductor. For example, epitaxial semi-metallic nanoparticles can donate carriers, pin Fermi levels, shorten electron–hole recombination times, enhance electron tunneling and increase scattering of phonons in semiconductor host layers. There are dozens of cubic semi-metallic group III–V rare-earth compounds that can potentially be grown as nanoparticles in the III–V semiconductors. The largest number of studies to date have involved nanocomposites of erbium-based compounds in arsenide and antimonide semiconductors. Their molecular beam epitaxy growth, properties and device applications will be reviewed.

© 2007 Elsevier B.V. All rights reserved.

PACS: 71.55.Eq

Keywords: A1. Nanostructures; A3. Molecular beam epitaxy; B1. Rare-earth compounds; B2. Semiconducting III–V materials

1. Introduction

The interaction between metals and semiconductors was studied since semiconductors were first investigated in the 19th century. Walter Schottky developed the first theory to explain the rectifying behavior at a metal/semiconductor interface in 1939 [1]. The advent of the improved growth technology, such as molecular beam epitaxy (MBE) [2], led to the exploration of a variety of material systems that exhibit more ideal versions of the classic metal/semiconductor interface. Depositions of metals by less controlled nonepitaxial techniques can result in polycrystalline material, interface oxides, dangling bonds, third phase material, and anisotropic diffusion of the metal into the semiconductor. These imperfections in the interface have significant and sometimes erratic effects on the behavior of the metal/semiconductor junction. Among the first investigations of high-quality epitaxial metal/semiconductor interfaces was Cho and Dernier's use of MBE to deposit in situ single-crystal aluminum on GaAs in the late 1970s [3]. They were able to produce Schottky diodes with lower

barriers and with more ideal behavior than that had been reported previously. In the 1980s, Tung and coworkers used MBE to epitaxially deposit metallic CoSi_2 and NiSi_2 on silicon [4–6]. In the past few decades, the ability to precisely control depositions and interfaces has led to more ideal semiconductor/metal interfaces and nanostructured composites consisting of metal particles imbedded within an epitaxial matrix of semiconductor.

1.1. ErAs on GaAs

Palmstrom et al. [7] began investigating semimetallic ErAs grown epitaxially on GaAs by MBE in 1988. ErAs as well as other rare-earth monoarsenides have several advantageous properties over other candidates for epitaxial GaAs/metal interfaces. ErAs is a very stable compound with a melting temperature of greater than 2500 °C. ErAs has a NaCl, rock salt, crystal structure with a lattice parameter of 5.74 Å 1.6% greater than GaAs and 2.1% smaller than InP. This crystal structure fits well with the zincblende structure of the group III-As semiconductors. As shown in Fig. 1(a), the arsenic sublattice is continuous over the interface between the zincblende semiconductor

*Corresponding author. Tel.: +805 893 7055.

E-mail address: micah@engr.ucsb.edu (M.P. Hanson).

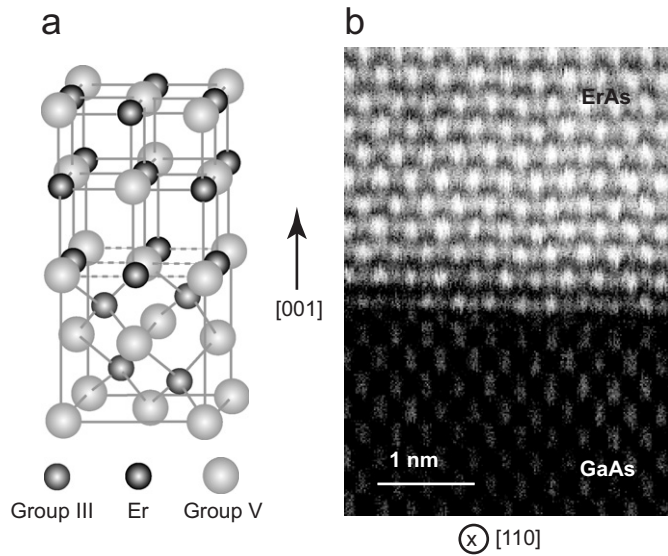


Fig. 1. (a) Model of rare-earth/group V rock-salt crystal structure on zincblende semiconductor. (b) STEM image of ErAs on GaAs [71].

and the rock-salt semi-metal. A detailed investigation of the ErAs/ $\text{In}_{0.53}\text{Ga}_{0.47}\text{As}$ and ErAs/GaAs interfaces via scanning transmission electron microscopy (STEM) was recently carried out by Klenov et al. [8] confirming this interface structure and measuring a slight increase in lattice spacing at the interface to accommodate the Er atoms in the first plane of ErAs. An STEM image of the ErAs/GaAs interface is shown in Fig. 1(b).

ErAs is just one of a family of rare-earth pnictides compounds. Guivarch et al. [9–12] investigated a variety of these types of materials including antimonide-based materials such as growth of ErSb and YbSb₂ on GaSb as well as phosphide-based ErP and ErPSb on InP. Like ErAs, these materials were found to grow epitaxially producing high-quality material.

1.2. Low-temperature-grown (LTG) GaAs

About the same time Palmstrom was beginning to investigate the epitaxy of ErAs on GaAs, the invention of LTG GaAs was made by Smith et al. [13]. The growth by MBE of GaAs at temperatures between 200 and 300 °C was found to result in a nonstoichiometric material in which excess arsenic is incorporated into GaAs. When the material is annealed, the arsenic migrates to form metallic clusters within the GaAs. It was found that this new metal/semiconductor composite material possessed several properties desirable for many applications. The resistivity of the LTG GaAs was much higher than traditionally grown GaAs. In addition, the recombination time for electrons and holes is much shorter, less than a picosecond, as mid-gap states from the arsenic precipitates and antisite defects trap carriers facilitating rapid non-radiative recombination. As a result of these two properties, LTG GaAs was found to be excellent materials for devices requiring an ultrafast photoelectric response. Two such devices are

Auston switches [14] and photomixers [15]. Both of these devices take advantage of the large and fast photoelectric response to produce and detect, in the case of Auston switches, radiation in the terahertz regime. Work on optimizing the LTG GaAs material and structure for photomixers was carried out at UCSB in the late 1990s [16].

1.3. Er-doped III–V semiconductors

Much of the initial, as well as continuing research, for erbium-doped semiconductors was motivated by the desire to take advantage of the atomic 4f optical transition in trivalent erbium (Er^{3+}) in optoelectronic devices [17]. This transition occurs at 1.54 μm conveniently located in the low-loss region of optical silica fibers used in telecommunications. Initial studies of Er-doped GaAs showed the solubility limit around $7 \times 10^{17} \text{cm}^{-3}$ for typical MBE growth conditions above which ErAs precipitates formed within the GaAs matrix [18]. The size of these precipitates was found to depend on growth temperature, resulting in ErAs particles ranging from about 1.2–3 nm in diameter for samples grown between 550 and 605 °C [18,19]. These ErAs precipitates were found to be detrimental to the photoluminescence properties of both the 4f transition in the Er atoms and the inter-band transitions of the GaAs matrix making the material ill-suited for light emitting devices [19]. However, like the As precipitates in LTG GaAs, the ErAs particles were also shown to reduce the photo-generated carrier lifetime. Gupta et al. [20] measured carrier lifetimes of ~ 1 ps for GaAs doped with $5 \times 10^{19} \text{cm}^{-3}$ Er. In addition to investigating Er doping of GaAs, Sethi and Bhattacharya also investigated Er-doped InGaAs. They found the material to be very conductive for doping ranges from 1×10^{16} to $5 \times 10^{19} \text{cm}^{-3}$ with long carrier lifetimes in excess of 100 ps [19].

2. Er-V nanoparticles in III–V semiconductors

Building on the research of Palmstrom as well as the Er-doped GaAs work of Sethi and Bhattacharya, Kadow and Ibbetson investigated ErAs growth regime before the formation of a complete ErAs film [21–23]. In this regime, ErAs forms a discontinuous network of three-dimensional islands which can be then be epitaxially overgrown with GaAs to form a composite material containing semi-metallic ErAs particles within a GaAs matrix. The size, shape and density of these island particles could be controlled more easily with growth conditions [24,25] than the precipitates formed in Er-doped GaAs [18]. This composite material, formed by repeated layers containing ErAs islands overgrown with GaAs to form a superlattice, has a similar microstructure to the As clusters found in LTG GaAs [24,25]. It was found that in addition to similar microstructures LTG GaAs and the ErAs/GaAs composite material shared similar optoelectronic properties of short carrier lifetimes [23] and high dark resistivity [26]. Kadow

et al. [26,27] demonstrated photomixer performance on this type of material comparable to that of LTG GaAs. The benefit of ErAs/GaAs nanocomposites over that of LTG GaAs is that ErAs/GaAs structures can be grown at normal GaAs growth temperatures and materials parameters such as carrier lifetime can be controlled by relatively standard MBE techniques such as changing layer and deposition thickness rather than growth temperature and annealing temperature which is the case with LTG GaAs. The success of these experiments in GaAs motivated the interest in looking at other matrices particularly those with lower band gaps that would absorb at $1.55\ \mu\text{m}$ where there is a wealth of laser technology.

ErAs particles in InGaAs latticed matched to InP [28] and ErSb particles in GaSb [29] were investigated as lower band gap composites. While ErAs particles in GaAs produced a resistive material, ErAs particles in InGaAs were found to act as a dopant contributing electrons to the semiconductor. The concentration of electrons in the composite is determined by the size of the ErAs particles with smaller particles leading to higher electron concentrations. By delta doping, the layers containing the ErAs particles with acceptors such as beryllium, the electron concentration is reduced and the resistivity of the composite increased [30]. These beryllium-compensated ErAs/InGaAs superlattices can have electron–hole lifetimes shorter than 300 fs. The lifetimes can be tuned by adjusting the spacing of the layers of particles, the size of the particles, the beryllium compensation.

In ErSb/GaSb superlattices, the ErSb particles reduce the hole concentration in the unintentionally p-type GaSb. As was found for ErAs particles in InGaAs, the Fermi level of the composite material increases with respect to the band edges of the semiconductor as the particle size is reduced. However, since as-grown GaSb is unintentionally p-type smaller ErSb particles reduce the hole concentration in the composite resulting in more resistive material. ErSb/GaSb also can exhibit very short electron–hole lifetimes shorter than 300 fs. The electron–hole lifetimes were found to decrease with decreasing superlattice period and increasing ErSb particle size [31]. The shortest lifetimes were obtained for superlattices containing large ErSb particles grown at close layer spacings.

3. Applications for metal/semiconductor composites

The unique properties created by the interaction between metals and semiconductors has led to a variety of applications which take advantage of, or hope to take advantage of these properties. As previously mentioned, the mid-gap states of the metal can act as traps for electrons and holes, leading to fast electron–hole recombination. The Schottky barrier created by the interface between the metal and semiconductor can pin the Fermi level in the semiconductor. Depending on the materials system, the Fermi level of the metal may lie near the band edge of the semiconductor or in the middle of the gap. If

located in the middle of the gap, the metal particles can deplete the surrounding carriers and lead to a more resistive material. In the case in which the Fermi level is near the band edge, the metal can contribute electrons/holes to the semiconductor, acting as a dopant. The interfaces between the metal and semiconductor can scatter phonons, reducing thermal conductivity in the composite material. The free electrons bound within the metal by the semiconductor interface can also have significant effects on the optical properties. These electrons can oscillate with the electric field of incident light in certain resonance conditions. These oscillations can modify the propagation of light within the composite material and locally perturb the electric field in the semiconductor around the metal. All of these aspects have been or are currently being explored for a variety of applications.

3.1. Photomixers, switches and photodetectors

Photomixers, photoconductive switches and detectors based on metal/semiconductor composite materials all benefit from the mid-gap states and higher resistivities that result from metal inclusions in the semiconductor matrix. In all of these devices, a photoconductive medium is biased and illuminated with photons above the energy of the semiconductor band gap. The performance of the device is related to material properties of the photoconductive medium. The sensitivity of the device is dependent on the magnitude of the photocurrent that can be produced as well as the efficiency of the extraction of the photo-generated carriers. It is, therefore, desirable for the photoconductive material to have a high dark resistance and high electron mobility, allowing both maximum photocurrent and maximum bias. A higher bias can improve the extraction of photo-generated carriers through an increase in the acceleration of the carriers to the contacts/antenna. Materials in which the metal particles deplete the surrounding carriers and pin the Fermi level in the middle of the semiconductor band gap are therefore desirable for their higher resistivity. The high-quality semiconductor regions between the particles provide conduction paths that retain a relatively high electrical mobility. The speed of these devices is limited by the time it takes the photoconductive material to return to the dark, pre-illuminated, state. One way in which this can be engineered is by reducing the time required for electron–hole pairs to recombine. In metal/semiconductor composites, this is achieved through non-radiative recombination via the states of the metallic particles within the band gap.

Much of the initial work on MBE of metal/semiconductor composite materials was motivated by the development of materials for photomixers operating at terahertz frequencies. A photomixer is a biased photoconductive switch coupled to an antenna. An oscillating photocurrent is generated across the switch by illuminating the gap with two lasers of slightly differing frequencies. The lasers interfere with each other to produce intensity oscillations at

the difference frequency. The photocurrent tracks this oscillating intensity, driving current through the antenna to produce radiation at the difference frequency. The maximum terahertz frequency that can be reached is limited by the RC time constant of the structure and the photocarrier lifetime of the photoconductor. The most commonly used material for this application has been LTG GaAs [15,16]. More recently, ErAs particles in GaAs has been shown to be suitable for photomixing [21,26,27,32]. This material has the added advantage of more conventional MBE growth conditions.

While photomixers generate tunable coherent cw radiation out to terahertz frequencies, photoconductive switches [14], or Auston switches, produce an electromagnetic pulse containing a broad band of frequencies out to the terahertz regime. In the case of switches, a very short femtosecond laser pulse is incident on a biased photoconductive material. This produces a very short pulse of current that emits broadly in frequency space. Like the photomixer, it is advantageous for the photoconductive material to be highly resistive in the dark and able to support a high electric field. This allows a large change in current when the device is illuminated and therefore higher output power. Because of the similarities in properties required for both switches and photomixers, materials that make good photomixers also tend to make good switches. LTG GaAs is also one of the most widely used materials for photoconductive switches [33]. Likewise, GaAs containing ErAs particles has also been shown to produce good photoconductive switches [34].

In detecting the terahertz pulse from a switch, the oscillating electric field of the pulse provides the electric field that drives the current across a photoconductive gap. A femtosecond laser pulse illuminates the gap and is scanned through time with respect to the source pulse. The magnitude and direction of the THz pulse's electric field are mapped out over time by measuring the photocurrent at each pulse. In order to maximize sensitivity, the photoconductor should have high electron mobility to maximize photocurrent and short carrier lifetimes to temporally resolve the field. Recently, it has been shown that detectors fabricated from GaAs containing ErAs particles have much greater sensitivity than those made from LTG GaAs and radiation damaged silicon [35].

The high resistivity and short carrier lifetimes of some metal/semiconductor composites such as LTG GaAs have enabled fabrication of high-speed photodiodes and detectors [36–39]. The short carrier lifetimes allow the detectors to resolve very short picosecond pulses while the high resistivities permit high biases and large changes in photocurrent.

3.2. Tunnel junction applications

The gap states created by the metallic particle inclusions that are responsible for the rapid carrier recombination observed in many metal/semiconductor composites can

also be used to increase carrier recombination across a tunnel junction. Tunneling currents across a p–n junction were shown to increase when metallic particles are placed at the junction. The increased tunneling is a result of a two-step tunneling process in which electrons can tunnel into the metal particles from the conduction band then again out of the metal particles into the valence band. Both thin layers of LT GaAs and single layers of ErAs particles at p–n junctions were shown to increase tunneling [40,41]. The method of placing ErAs particles at the junction is more easily controlled than a layer of LTG GaAs, so that a single layer of particles can be placed exactly at the junction interface. These ErAs particles placed at p–n junctions were demonstrated to improve performance in multijunction solar cells by reducing the voltage lost across the tunnel junctions between cells [42]. These tunnel junctions have also been employed by Dohler and coworkers in a photomixer based on ballistic travel across a series of pin diodes connected together with tunnel junctions [43–49].

3.3. Thermoelectrics

Thermoelectric materials require both high electrical conductivity and low thermal conductivity. These are often difficult properties to achieve simultaneously because mechanisms that scatter phonons also tend to scatter electrons. Recently, it has been found that because the Fermi level of small ErAs particles lies near the conduction band of InGaAs, the particles donate electrons to the InGaAs matrix [50]. There is sufficient InGaAs material between the ErAs particles to allow conduction paths around the scattering centers so that high electrical carrier mobility is maintained. The ErAs particles are of sufficient size and spacing to scatter medium wavelength phonons leading to a substantial reduction in thermal conductivity. As a result, it was demonstrated that the ErAs particles in InGaAs may prove to be a very efficient thermoelectric material for power generation [51–54]. An analogous p-type material such as ErSb particles in GaSb [29] may provide the opportunity to produce a p-type leg for a thermoelectric cell.

3.4. Plasmon devices

The electrons within the metallic particles are bound by the surrounding semiconductor. When an oscillating electric field, in the form of light, is incident on the particle, the electrons are displaced. The edges of the particle build up charge and act as a restoring force on the electrons. Under resonant conditions, these electrons oscillate coherently resulting in oscillating electromagnetic fields. These resonant oscillations are called localized surface plasmons to distinguish them from propagating surface plasmons that can occur on metal surfaces. The oscillating charge results in strong absorption at the

resonance condition and enhancement of the local electric field around the particles.

The vast majority of the work on applications for surface plasmons was performed on particles suspended in liquids or on the surface of substrates [55]. Typically, small Ag and Au particles are used which often have resonances in the UV and visible. The most well-developed application has been surface enhanced Raman spectroscopy [56] in which the enhanced local fields near metallic particles, due to the plasmon resonance, boost the spectroscopic signal of near by molecules. Embedding metal particles in higher index materials such as semiconductors is known to push the resonance toward the infrared [57–60] and provide the possibility of integrating plasmon-based functions with traditional semiconductor devices. Applications more relevant to metal/semiconductor composites such as photodetectors [61,62] and solar cells [63–65] are also being investigated in an effort to use the field enhancement associated with the plasmon resonance to increase absorption [66]. Emerging applications in nano-optics [67] attempt to take advantage of the ability of surface plasmons to confine the electric field oscillations in an area much smaller than the wavelength of the light.

The growth compatibility of the rare-earth pnictides with III–V semiconductors makes these materials good candidates for incorporating surface plasmon effects into semiconductor devices. Resonances for ErAs particles in GaAs were shown to be tunable from 1.3 to 2.5 μm based on the growth conditions [59]. For ErSb particles in GaSb, the resonances are shifted to longer wavelengths from 2.5 to 4 μm depending on growth conditions [60]. For dense distributions of larger particles, the absorption due to the surface plasmon resonance can exceed that of the cross band gap absorption of the semiconductor matrix.

3.5. Contacts and diodes

Perhaps the most basic and well-studied interaction between metals and semiconductors is the use of the metal–semiconductor interfaces as either rectifying Schottky diodes or Ohmic electrical contacts. The ability to grow epitaxial metals such as ErAs and ErSb without the creation of interfacial third phases or oxides may lead to improvements in both contacts and diodes. Zimmerman et al. [68] have demonstrated highly tunable barrier heights of ErAs–InAlGaAs junctions based on the interface type and composition of the semiconductor. These high-quality diodes are being investigated for high radio frequency (rf) detection due to their very low $1/f$ noise [69,70]. In addition, extrapolation of the barrier dependence found by Zimmerman to high In compositions may lead to near ideal Ohmic contacts for ErAs on InAs. Meanwhile, ErSb contacts on GaSb may prove to be an equivalently good p-type contact.

4. Summary

The growth compatibility of rare-earth pnictides with many III–V semiconductors allows the construction of various types of epitaxial metal/semiconductor heterostructures. Various electrical and optical properties of the composite material can be influenced by the interaction between the two dissimilar materials. This interaction is mediated by the band alignment between metal and semiconductor and is determined by the shape and size of the particle as well as the matrix semiconductor. Metallic particles incorporated in a bulk semiconductor can result in composite material with very different properties than either of constituent materials. These composite materials may possess faster electron–hole recombination, lower thermal conductivity, increased or decreased carrier concentrations, and modified absorption spectra due to plasma resonances. These properties may result, or have resulted, in improvements in a variety of applications including photodetectors, terahertz sources, electron barriers/insulating layers, dopant layers, and thermoelectrics. Layers of metallic nanoparticles can also be strategically placed within a structure, such as the interface of a p–n junction. In this case, the particles can mediate the transport across the junction, increasing the tunneling current or perhaps modifying spin states if a magnetic material is used. Finally, layers of epitaxially grown rare-earth pnictides on semiconductors can result in superior low defect interfaces and high-quality single-crystal semimetals. These low defect interfaces can be used to produce low-noise Schottky diodes for microwave detection, or low resistance Ohmic contacts.

Acknowledgments

The authors thank Dmitri Klenov for the TEM image shown in this paper. This work was supported by the Office of Naval Research, Defense Advanced Research Projects Agency, and the National Science Foundation.

References

- [1] W. Schottky, *Phys* 113 (1939) 367.
- [2] A.Y. Cho, *J. Appl. Phys.* 42 (1971) 2074.
- [3] A.Y. Cho, P.D. Dernier, *J. Appl. Phys.* 49 (1978) 3328.
- [4] R.T. Tung, J.C. Bean, J.M. Gibson, J.M. Poate, D.C. Jacobson, *Appl. Phys. Lett.* 40 (1982) 684.
- [5] R.T. Tung, *Mater. Chem. Phys.* 32 (1992) 107.
- [6] R.T. Tung, F. Schrey, *Appl. Phys. Lett.* 54 (1989) 852.
- [7] C.J. Palmstrom, N. Tabatabaie, S.J. Allen, *Appl. Phys. Lett.* 53 (1988) 2608.
- [8] D.O. Klenov, J.M. Zide, J.D. Zimmerman, A.C. Gossard, S. Stemmer, *Appl. Phys. Lett.* 86 (2005).
- [9] A. Guivarch, A. Lecorre, P. Auvray, B. Guenais, J. Caulet, Y. Ballini, R. Guerin, S. Deputier, M.C. Leclanche, G. Jezequel, B. Lepine, A. Quemerais, D. Sebilliau, *J. Mater. Res.* 10 (1995) 1942.
- [10] A. Guivarch, Y. Ballini, P. Auvray, J. Caulet, M. Minier, G. Dupas, G. Ropars, *J. Appl. Phys.* 74 (1993) 6632.

- [11] A. Guivarch, Y. Ballini, Y. Toudic, M. Minier, P. Auvray, B. Guenais, J. Caulet, B. Lemerdy, B. Lambert, A. Regreny, *J. Appl. Phys.* 75 (1994) 2876.
- [12] A. Guivarch, J. Caulet, A. Lecorre, *Electron. Lett.* 25 (1989) 1050.
- [13] F.W. Smith, A.R. Calawa, C.L. Chen, M.J. Manfra, L.J. Mahoney, *IEEE Electron. Dev. Lett.* 9 (1988) 77.
- [14] D.H. Auston, K.P. Cheung, J.A. Valdmanis, D.A. Kleinman, *Phys. Rev. Lett.* 53 (1984) 1555.
- [15] E.R. Brown, F.W. Smith, K.A. McIntosh, *J. Appl. Phys.* 73 (1993) 1480.
- [16] Andrew W. Jackson, Low-temperature-grown GaAs photomixers designed for increased terahertz output power, Ph.D. Thesis, University of California, Santa Barbara, 1999.
- [17] A.J. Kenyon, *Prog. Quantum Electron.* 26 (2002) 225.
- [18] I. Poole, K.E. Singer, A.R. Peaker, A.C. Wright, *J. Crystal Growth* 121 (1992) 121.
- [19] S. Sethi, P.K. Bhattacharya, *J. Electron. Mater.* 25 (1996) 467.
- [20] S. Gupta, S. Sethi, P.K. Bhattacharya, *Appl. Phys. Lett.* 62 (1993) 1128.
- [21] C. Kadow, Self-assembled ErAs islands in GaAs for photomixer devices, Ph.D. Thesis, University of California, Santa Barbara, 2000.
- [22] D.R. Schmidt, A.G. Petukhov, M. Foygel, J.P. Ibbetson, S.J. Allen, *Phys. Rev. Lett.* 82 (1999) 823 LP.
- [23] C. Kadow, S.B. Fleischer, J.P. Ibbetson, J.E. Bowers, A.C. Gossard, J.W. Dong, C.J. Palmstrom, *Appl. Phys. Lett.* 75 (1999) 3548.
- [24] C. Kadow, J.A. Johnson, K. Kolstad, A.C. Gossard, *J. Vac. Sci. Technol. B* 21 (2003) 29.
- [25] C. Kadow, J.A. Johnson, K. Kolstad, J.P. Ibbetson, A.C. Gossard, *J. Vac. Sci. Technol. B* 18 (2000) 2197.
- [26] C. Kadow, A.W. Jackson, A.C. Gossard, S. Matsuura, G.A. Blake, *Appl. Phys. Lett.* 76 (2000) 3510.
- [27] C. Kadow, A.W. Jackson, A.C. Gossard, J.E. Bowers, S. Matsuura, G.A. Blake, *Physica E* 7 (2000) 97.
- [28] D.C. Driscoll, M.P. Hanson, E. Mueller, A.C. Gossard, *J. Crystal Growth* 251 (2003) 243.
- [29] M.P. Hanson, D.C. Driscoll, C. Kadow, A.C. Gossard, *Appl. Phys. Lett.* 84 (2004) 221.
- [30] D.C. Driscoll, M.P. Hanson, A.C. Gossard, *J. Appl. Phys.* 97 (2005).
- [31] M.P. Hanson, D.C. Driscoll, J.D. Zimmerman, A.C. Gossard, E.R. Brown, *Appl. Phys. Lett.* 85 (2004) 3110.
- [32] J.E. Bjarnason, T.L.J. Chan, A.W.M. Lee, E.R. Brown, D.C. Driscoll, M. Hanson, A.C. Gossard, R.E. Muller, *Appl. Phys. Lett.* 85 (2004) 3983.
- [33] D.C. Look, *Thin Solid Films* 231 (1993) 61.
- [34] Z.D. Taylor, E.R. Brown, J.E. Bjarnason, M.P. Hanson, A.C. Gossard, *Opt. Lett.* 31 (2006) 1729.
- [35] J.F. O'Hara, J.M.O. Zide, A.C. Gossard, A.J. Taylor, R.D. Averitt, *Appl. Phys. Lett.* 88 (2006).
- [36] K.G. Gan, J.W. Shi, Y.H. Chen, C.K. Sun, Y.J. Chiu, J.E. Bowers, *Appl. Phys. Lett.* 80 (2002) 4054.
- [37] Y.J. Chiu, S.B. Fleischer, J.E. Bowers, *IEEE Photonic. Technol. Lett.* 10 (1998) 1012.
- [38] Y.J. Chiu, S.B. Fleischer, D. Lasaosa, J.E. Bowers, *Appl. Phys. Lett.* 71 (1997) 2508.
- [39] Y. Chen, S. Williamson, T. Brock, F.W. Smith, A.R. Calawa, *Appl. Phys. Lett.* 59 (1991) 1984.
- [40] D.E. Brehmer, K. Zhang, C.J. Schwarz, S.P. Chau, S.J. Allen, J.P. Ibbetson, J.P. Zhang, A.G. Petukhov, C.J. Palmstrom, B. Wilkens, *Solid-State Electron.* 40 (1996) 241.
- [41] P. Pohl, F.H. Renner, M. Eckardt, A. Schwanhauser, A. Friedrich, O. Yuksekdog, S. Malzer, G.H. Dohler, P. Kiesel, D. Driscoll, M. Hanson, A.C. Gossard, *Appl. Phys. Lett.* 83 (2003) 4035.
- [42] J.M.O. Zide, A. Kleiman-Shwarstein, N.C. Strandwitz, J.D. Zimmerman, T. Steenblock-Smith, A.C. Gossard, A. Forman, A. Ivanovskaya, G.D. Stucky, *Appl. Phys. Lett.* 88 (2006).
- [43] G.H. Dohler, M. Eckardt, A. Schwanhauser, F. Renner, L. Robledo, A. Friedrich, P. Pohl, S. Malzer, P. Kiesel, D. Driscoll, M. Hanson, A. C. Gossard, in: 2002 Conference on Optoelectronic and Microelectronic Materials and Devices, IEEE, Sydney, NSW, Australia, 2002, p. 275.
- [44] G.H. Dohler, F. Renner, O. Klar, M. Eckardt, A. Schwanhauser, S. Malzer, D. Driscoll, M. Hanson, A.C. Gossard, G. Loata, T. Loffler, H. Roskos, *Semicond. Sci. Technol.* 20 (2005) S178.
- [45] M. Eckardt, A. Schwanhauser, F. Renner, L. Robledo, A. Friedrich, P. Pohl, P. Kiesel, S. Malzer, G.H. Dohler, D. Driscoll, M. Hanson, A.C. Gossard, *THz 2002*, in: 2002 IEEE Tenth International Conference on Terahertz Electronics Proceedings, IEEE, Cambridge, UK, 2002, p. 151.
- [46] M. Eckardt, A. Schwanhauser, F. Renner, L. Robledo, A. Friedrich, P. Pohl, P. Kiesel, S. Malzer, G.H. Dohler, D. Driscoll, M. Hanson, A.C. Gossard, *Elsevier. Physica A* 17 (2003) 629.
- [47] S. Malzer, M. Eckardt, A. Schwanhauser, F. Renner, A. Friedrich, P. Pohl, D. Driscoll, M. Hanson, P. Kiesel, A. C. Gossard, G.H. Dohler, in: Proceedings of the 2003 SBMO/IEEE MTT-S International Microwave and Optoelectronics Conference—IMOC 2003, IEEE, Brazil, 2003, p. 69.
- [48] F. Renner, M. Eckardt, A. Schwanhauser, O. Klar, S. Malzer, G.H. Dohler, G. Loata, T. Loffler, H. Roskos, M. Hanson, D. Driscoll, A.C. Gossard, *Phys. Stat. Sol. a-Applications and Materials Science* 202 (2005) 965.
- [49] F.H. Renner, O. Klar, S. Malzer, D. Driscoll, M. Hanson, A.C. Gossard, G. Loata, T. Loffler, H. Roskos, G.H. Dohler, *PHYSICS OF SEMICONDUCTORS: 27th International Conference on the Physics of Semiconductors—ICPS-27*, AIP, Flagstaff, AZ, USA, 2005, p. 1220.
- [50] D.C. Driscoll, M. Hanson, C. Kadow, A.C. Gossard, *Appl. Phys. Lett.* 78 (2001) 1703.
- [51] W. Kim, J. Zide, A. Gossard, D. Klenov, S. Stemmer, A. Shakouri, A. Majumdar, *Phys. Rev. Lett.* 96 (2006).
- [52] W. Kim, S.L. Singer, A. Majumdar, D. Vashaee, Z. Bian, A. Shakouri, G. Zeng, J.E. Bowers, J.M.O. Zide, A.C. Gossard, *Appl. Phys. Lett.* 88 (2006).
- [53] G.H. Zeng, J.E. Bowers, J.M.O. Zide, A.C. Gossard, W. Kim, S. Singer, A. Majumdar, R. Singh, Z. Bian, Y. Zhang, A. Shakouri, *Appl. Phys. Lett.* 88 (2006).
- [54] J.M. Zide, D.O. Klenov, S. Stemmer, A.C. Gossard, G. Zeng, J.E. Bowers, D. Vashaee, A. Shakouri, *Appl. Phys. Lett.* 87 (2005).
- [55] E. Hutter, J.H. Fendler, *Adv. Mater.* 16 (2004) 1685.
- [56] T. Vo-Dinh, *Trends in Anal. Chem.* 17 (1998) 557.
- [57] D.D. Nolte, *J. Appl. Phys.* 76 (1994) 3740.
- [58] H. Mertens, J. Verhoeven, A. Polman, F.D. Tichelaar, *Appl. Phys. Lett.* 85 (2004) 1317.
- [59] E.R. Brown, A. Bacher, D. Driscoll, M. Hanson, C. Kadow, A.C. Gossard, *Phys. Rev. Lett.* 90 (2003) 077403.
- [60] M.P. Hanson, D.C. Driscoll, E.R. Brown, A.C. Gossard, in: *Physics of Semiconductors: 27th International Conference on the Physics of Semiconductors—ICPS-27*, AIP, Flagstaff, AZ, USA, 2005, p. 845.
- [61] E.L. Chen, S.Y. Chou, *Appl. Phys. Lett.* 70 (1997) 753.
- [62] H.R. Stuart, D.G. Hall, *Appl. Phys. Lett.* 69 (1996) 2327.
- [63] S. Hayashi, K. Kozaru, K. Yamamoto, *Solid State Commun.* 79 (1991) 763.
- [64] T. Kume, S. Hayashi, K. Yamamoto, *Jpn. J. Appl. Phys. Part 1-Regular Papers Short Notes Rev. Papers* 32 (1993) 3486.
- [65] M. Westphalen, U. Kreibitz, J. Rostalski, H. Luth, D. Meissner, *Solar Energy Mater. Solar Cells* 61 (2000) 97.
- [66] D.M. Schaadt, B. Feng, E.T. Yu, *Appl. Phys. Lett.* 86 (2005).
- [67] W.L. Barnes, A. Dereux, T.W. Ebbesen, *Nature* 424 (2003) 824.
- [68] J.D. Zimmerman, E.R. Brown, A.C. Gossard, *J. Vac. Sci. Technol. B* 23 (2005) 1929.
- [69] A.C. Young, J.D. Zimmerman, E.R. Brown, A.C. Gossard, *Appl. Phys. Lett.* 87 (2005).
- [70] A.C. Young, J.D. Zimmerman, E.R. Brown, A.C. Gossard, *Appl. Phys. Lett.* 88 (2006).
- [71] D.O. Klenov, J.M. Zide, J.D. Zimmerman, A.C. Gossard, S. Stemmer, *Appl. Phys. Lett.* 86 (2005) 241901.